

# An Intelligent Thermal Sensing System for Automatic, Quantitative Assessment of Motion Training in Lower-Limb Rehabilitation

Rui Ma, and Fei Hu, *Member, IEEE*

**Abstract**—Many patients who suffer from the paralysis can recover body functions by taking appropriate rehabilitation training. This paper presents an intelligent, low-cost sensing system which can automatically generate quantitative measures of the quality of human motions. This study aims to develop a home-oriented cyber-physical system (CPS) to help the patients improve their motion coordination capability via physical training. The system provides quantitative evaluation for the performed motions. The measures evaluated by the system include the motion style of the legs, the periodicity of the foot trajectory, and the foot balance level, which are recommended by the physical therapists. The motions of legs and feet are recorded by the thermal camera, and the plantar pressure is measured by the insole pressure sensors. We have developed innovative algorithms to extract the leg skeletons from the thermal images, and to implement motion signal auto-segmentation, recognition and analysis for the above mentioned measures. The experimental results have verified that the proposed system could efficiently acquire and analyze the lower-limb motion information.

**Index Terms**—Rehabilitation, physical therapy, motion segmentation, recognition, thermal camera, pressure sensor.

## I. INTRODUCTION

**R**ECOVERY from a stroke or a spinal cord injury is difficult and could be a life-long process. Many patients can improve their motion functions after receiving carefully arranged physical training. Nowadays patients typically go to hospitals or facilities for rehabilitation. The nurses or therapists are needed in the programs to guide and correct the patients' training. The labor costs are thus very high. For example, the cost of physical therapy for stroke patients in the United States is about \$28 billion per year [1], and this number keeps going up in modern society.

One way to alleviate the medical burdens is to use intelligent rehabilitation systems to automatically recognize the patient's motions, and provide real-time evaluation and feedback. Today there are various sensing systems as well as machine learning techniques for systems. Unlike the general applications (such as smart homes) which coarsely recognize the human motions, the sensing system for rehabilitation training needs to recognize the motion of specific limbs or body parts with fine resolution. Today wearable inertial sensors [2], general cameras [3] and Microsoft Kinects [4], are the typical sensing systems used for this purpose.

The authors are with the Department of Electrical and Computer Engineering, University of Alabama, Tuscaloosa, AL 35487, USA. (email: rma3@crimson.ua.edu, Corresponding author: Fei Hu, fei@eng.ua.edu). Work supported by U.S. NSF CNS-1335263, CNS-1059212, and IIS-0915862.

Manuscript finished in May 10, 2015.

In this research, we regard a complete human motion as a series of static postures (with time). Wearable sensors can detect the dynamic motion signals, but they typically capture the changes of the posture (such as acceleration values), instead of the concrete posture image itself. Thus they have limitations when the measurement of the human limbs' absolute positions is desired. For example, one issue we concern is that if the patient's knee is raised high enough in the training. The positions of the knee, thigh, and foot cannot be captured via existing wearable sensors such as accelerometers since they do not record the image data. The cameras and depth sensors (such as Microsoft Kinect) can capture the image. However, general cameras are limited by the illumination conditions and the obstacles. MS Kinects cannot accurately capture the images within a short distance (less than 1 meter). Although some special algorithms can be applied to overcome those limits, they typically involve high computation cost.

In our image sensing system, we have used the thermal camera, which has the advantages of general cameras, but has no limitations in illumination and background since it takes the thermal images. It needs much less effort to extract the human subject from the images. In home-based rehabilitation systems, the thermal camera is desired to have low price, reasonable resolution, and small size. Most of the thermal cameras on the market are huge and expensive. The system Therm-App [7] wireless thermal camera that we used has a size smaller than a cell phone, costs less than \$1K, and can be connected to any Android platforms.

Many machine learning techniques can be used for recognizing the human motions. Most of those methods either extract the features from the motions, or perform the motion recognition by directly comparing the similarity of motion series. For the recognition of continuous motion data, segmenting the motion series is a necessary step. And segmentation and recognition of motion series are actually interrelated. The segmentation methods include supervised methods [9], [10] and unsupervised methods [12]. The feature-guided methods may lose some important raw information because the motion is represented by the extracted features. The unsupervised methods have large uncertainty in the segmentation process.

The contributions of our work include (1) the integrated sensing system for home-oriented rehabilitation training, consisting of a low-cost mobile thermal camera and the wireless thin film pressure sensors as shown in Fig. 1; and (2) the corresponding novel algorithms for real-time motion analysis:

(a) The fast skeleton extraction algorithm for the thermal

image data.

(b) The Peak Match Time Warping (PMTW) algorithm for accurate recognition and auto-segmentation of the motion series. It reduces the computation time of warping path search used in conventional DTW schemes. It can avoid mismatches between the time series containing peaks and has strong ability to resist data noise.

(c) The Scored Time-Delay Embedding (STDE) for periodicity analysis of the motion series. Few related studies have been reported in this area.

(d) Foot balance measurement. The Fourier power spectrum of the plantar pressure is used to provide the foot balance status of the patient, which is also an important rehabilitation progress metric.

The rest of the paper is organized as follows. Section II briefs the related work. In Section III we will introduce the architecture of our sensing system and the measures to be considered in rehabilitation. Then we detail our proposed algorithms for segmentation, recognition and analysis of the motion data in Section IV. Section V presents the experimental results. And Section VI concludes the paper.

## II. RELATED WORK

We will discuss the related studies in terms of hardware and software designs that are close to our system.

### A. Hardware

Up to this point, the inertial sensor, video camera, MS Kinect, and marker based motion capture system are the most popular sensing hardware units for human motion detection.

The inertial sensors mainly include accelerometers and gyroscopes. Hsu et al. [2] have used inertial sensors for stride detection and gait cycle decomposition to analyze to gait pattern and balance level. However, inertial signals can accumulate the displacement errors, and cannot capture the comprehensive human postures since they cannot “see” the real images of human body.

Video camera can “see” the body skeleton. For example, Ayase et al. [3] have built an general camera system for at-home fitness exercise guidance. General cameral system can record the postures of human motions. However, video/image processing often consumes huge computing resources when extracting the limb motions. It is also limited by the illumination conditions and background obstacles, and often has a limited field of view. MS Kinect captures depth images and has been used in medical applications. But its signals can be blocked by the obstacles near the subject. For example, Ar et al. [4] have built a recognition system with home-based physiotherapy exercises based on MS Kinect. Marker-based system is usually used in research and film industry. It uses cameras to detect the markers on the body joints. Das et al. [5] have performed full-body motion capture for Parkinson patients through a marker-based Vicon system. Marker-based system captures the most accurate human posture in the existing techniques. But its high cost makes it not suitable to home-oriented applications.

### B. Software

Some proposed algorithms used simple signal features for the segmentation of motion series. In the work [2] they segment the gait cycles by examining the changing points of the sensor signals. Some other works used more accurate segmentation and recognition methods. For example, Lin et al. [9] have proposed an online segmentation scheme by using zero-velocity crossings and velocity peaks as features, and Hidden Markov Model as recognition method. Lin’s method has applied a frequency filter, and can thus filter out the fast or slow motions. Frank et al. [10] have used Time-Delay Embedding (TDE) method to recognize the time series. The TDE projection of the original signals may lose much information of the motion series.

Another popular method for the recognition of the time series is Dynamic Time Warping (DTW). It can calculate the similarity between two time series with different lengths, but the DTW alignment of two time series only considers the amplitudes of time series. It will match the points with close amplitudes together even one point is at the peak and the other is at the valley. Keogh et al. [11] have proposed a Derivative DTW (DDTW) that alleviates the above mentioned mismatch problem by introducing the first order derivative of the time series. Zhou et al. [12] have developed a hierarchical segmentation (HACA) based on Dynamic Time-Alignment Kernel method (DTAK) and k-means clustering. It uses an unsupervised learning, but has large computation overhead and is sensitive to initial values and parameters.

Regarding the analysis of the periodicity of motion series, very few studies have targeted on the quantification of periodicity. Liu et al. [13] have used Fourier spectrum power to determine the periodicity of image series. However, the Fourier spectrum power can only determine the existence of sinusoid components, and thus is not a good measure of periodicity for more complex signals.

## III. SENSING SYSTEM OVERVIEW

The overview of the system is shown in Fig. 1. In this work we focus on measuring three aspects: the motion of raising legs, the periodicity of the motion trajectory, and the foot pressure balance. The proposed sensing system is designed to acquire these measures in lower-limb motions, but it can also be used for other detections such as upper-limb motions.

### A. Rehabilitation Measures

American Physical Therapy Association (APTA) has defined 54 outcome measures [14] for the patients with stroke in rehabilitation. The measures such as “6 minute walk” and “Berg Balance Scale” are proper assessment of the patient’s speed, strength, endurance, etc. However, those measures mostly reveal the final training effects without descriptions of the entire process. For example, does the patient’s motion show good periodical patterns? In this work, we will consider some other measures that can reveal the dynamics of the patient’s motions. Especially, we will target the following 3 measures:

(1) Height of raising legs. Jaffe et al. [8] have found that the individuals with post-stroke hemiplegia have an obvious

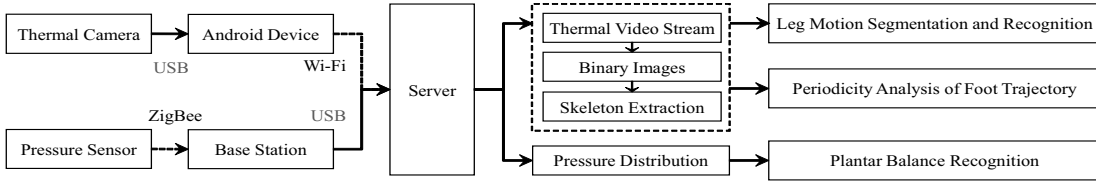


Fig. 1. The sensing system architecture.

improvement in gait velocity and endurance by taking the training of stepping over obstacles. As a matter of fact, raising legs is not a simple training step. It requires good coordination and enough strength for most of the leg muscles.

(2) Periodicity. The repeatability of the motion trajectory is considered as an important measure of the patient's capability of controlling the limbs. For normal people, it takes no effort to repeat the walking cycles. But for the stroke patients, it is already difficult for them to move the limbs, not to mention moving with the same pattern each time. By training them to walk with high repeatability we can help them to improve the control of the leg muscles.

(3) Foot balance. For this measure, we focus on the distribution of the plantar pressure. The imbalance of pressure between two feet or within one foot can tell which part of the foot the subject intends to use: is it right/left leg, inside/outside foot, front foot, or heel? These parameters are helpful to correct the patient's gaits.

## B. Sensing System

The sensing system includes the mobile thermal camera and the wireless pressure sensors.

(1) The thermal camera obtains the thermal video stream of the subject, and sends it to the server through an Android device such as a cell phone with Wi-Fi. The thermal images of the video stream are converted to B&W images, and the background in the images is subtracted. The skeleton model of the detected lower limbs is then extracted out from the B&W images for later use.

(2) The wireless pressure sensor nodes detect the plantar pressure of both feet, and send the data to the server via ZigBee-based wireless protocol. The pressure distribution is obtained by searching the peak values in the power spectrum of the pressure sensor signals.

The server processes all the sensor data to recognize and evaluate the subject's motion patterns as shown in Fig. 1.

## IV. LOWER LIMB MOTION ANALYSIS

The motion analysis of the lower limbs is composed of three parts: (1) the recognition and segmentation of the motion series, (2) the quantification of the periodicity of the motion trajectory, and (3) the foot balance analysis. First, the thermal images from the camera are processed to obtain the human skeleton model. Second, PMTW algorithm is applied to the skeleton data for motion segmentation and recognition. Third, STDE algorithm is applied to the skeleton data for periodicity assessment. Fourth, the pressure distribution obtained from the pressure sensors are used to analyze the foot balance of walking subject.

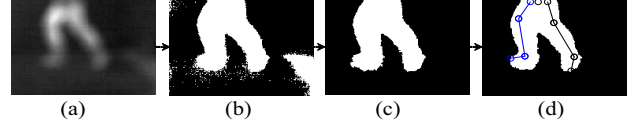


Fig. 2. The skeleton extraction of lower limbs from a thermal image: (a) raw image; (b) B&W image; (c) noise reduction; (d) skeleton extraction.

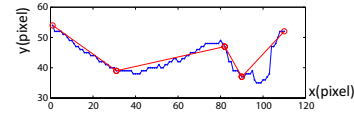


Fig. 3. The segmented linear regression of the edge of a leg taken from the thermal image.

### A. Skeleton Extraction from Thermal Image

The thermal camera only requires simple noise reduction to subtract the background and obstacles as shown in Fig. 2. We have developed a fast skeleton extraction algorithm for the given B&W images, based on the segmented linear regression. The algorithm includes the following three steps: (1) The edge of the extracted subject is taken out as a curve to be processed. (2) The curve is scanned through to find the changing points. (3) The changing points are moved in parallel inside the leg silhouette to become the skeleton joints. The curve is fitted by the segmented straight lines based on the detected changing points, as shown in Fig. 3. They are determined by the minimum error between the curve and the segmented lines. The overall error function is given by

$$ERR = \sum_{i=1}^n (1 - w_i) \times MSE_i + w_i / l_i, \quad (1)$$

Where  $w_i$  is the weighting factor,  $MSE$  is the mean square error, and  $l_i$  is the length of the segmented line.  $n$  is the number of segments. In this case, there are four segmented lines, thus  $n = 4$ . The objective function minimizes the overall error by choosing the weighted  $MSE_i$  and  $l_i$ .

We can set up the value of  $l_i$  based on certain prior knowledge. If the range of length between skeletons is known, we can set up the value of  $l_i$  in this range and assign a relatively large weighting to it, such that the objective function can converge quickly. The above method can be also used for skeleton extraction of human arms and other body parts.

### B. Motion Recognition

Recognition of the motion series can be performed based on the extracted lower limb skeleton data. Two problems need to be solved to recognize the motion series: (1) calculating the

similarity between different motion series; (2) segmentation of the motion series.

1) *General DTW Method*: The motion series may differ in length. The similarity between different vectors can be calculated directly. However, it is challenging to define the similarity between motion series with different lengths. A widely used solution for this problem is DTW. It calculates a similarity matrix for two series, and then searches for an optimal warping path with the maximal cumulative similarity.

2) *Proposed PMTW-based Approach*: Most of the human motions contain positive and negative peak patterns. We thus developed a Peak Match Time Warping (PMTW) based scheme to calculate the similarity between two time series. The series alignment in PMTW is based on the matching of the peaks. It can avoid DTW's singularity and mismatching issues, and also avoids the search of the optimal warping path. The procedure of PMTW algorithm is as follows:

- (a) Finding the peaks. The time series with noise typically contains small noise peaks everywhere. A popular solution is to use frequency filter, but it is not efficient in our applications because human motions may have different speed with the same frequency as the noise. We have developed a new algorithm "amplitude smoothing" to get rid of the noise and find the peaks. First, it detects all the peaks including the noise in the signal. Second, if the amplitude of a peak is under a threshold, it will be replaced by the average of its neighboring two peaks. The averaging operation is implemented iteratively until the amplitudes of all peaks are above the threshold. In our tested cases, at most 5 iterations of computation is enough to eliminate all the noise. And the computational cost of our amplitude smoothing with 4 iterations is the same as using one discrete Fourier transform for the same series. The MATLAB functions "tic" and "toc" are used to calculate the time they consume. Fig. 4 shows the detected peaks in two artificial signals with noise.
- (b) Matching the peaks and warping the series. All the peaks obtained in the last step will be matched. And the rest of points in the series will be equally aligned between the neighboring two peaks, as shown in Fig. 4. This warping does not need to search for the optimal path since the main structure of the warping has already been determined by the matched peaks. If the testing series having different peak pattern from the template series, the unmatched peaks will be aligned to the end of the series. In Fig. 4 (c), since PMTW cannot find the matched peaks, it gives a low similarity score; but in Fig. 4 (d), DTW tries to align the testing points with their similar counterpoints, even the alignment is totally wrong. This can result in a high similarity score between two dissimilar series. Therefore, using DTW to recognize motion series can sometimes generate wrong matching results.

3) *Segmentation of Motion Series*: The segmentation of time series based on PMTW is a supervised learning process. It finds the segments with matched peaks and high similarity with the template series. The series that is not matched with the template library will not be recognized. The segmentation

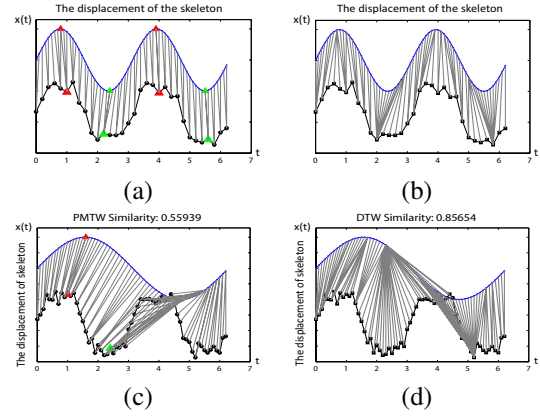


Fig. 4. Comparison between PMTW and DTW: (a) PMTW alignment and (b) DTW alignment; (c) PMTW similarity and (d) DTW similarity

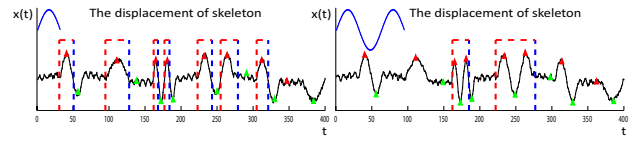


Fig. 5. The segmentation of synthetic signals.

starts from the beginning to the end of the input series to find all the matched segments, based on the following main steps:

- (a) Find all the peaks in the input motion series.
- (b) Locate the first group of matched peaks.
- (c) Initializing the starting point and ending point. Set starting point at the first matched peak, and ending point at the last matched peak.
- (d) Move starting point backward until encountering the previous peak, and then calculate the PMTW score. Pick the point with the largest score as the final starting point.
- (e) Move the ending point forward. Do similar thing as last step to find the final ending point.
- (f) Go forward to search for the next group of matched peaks.

An example of the segmentation of a long synthetic series containing different patterns of peaks is shown in Fig. 5. It can be seen that the series matched with different templates are recognized and segmented from the long series, even they are disturbed by noise and different speeds.

### C. Periodicity of Trajectory

Regarding the period detection, Fourier Transform is the first consideration. However, frequency analysis can only find out the existence of sinusoid signals. Therefore, it cannot accurately measure the quality of periodicity.

1) *TDE-based Scheme*: TDE is a technique of reconstructing the dynamics of time series. Suppose there is a dynamical system with its state at time  $t$  as  $s_t \in R^d$ , and all these states belong to the phase space. These states cannot be directly measured, and the dimension of the phase space  $d$  is also unknown. But we have the observation of the system  $o_t = \alpha(s_t) \in R$ , where  $\alpha$  is a smooth observation function. According to Takens Embedding Theorem, the system states

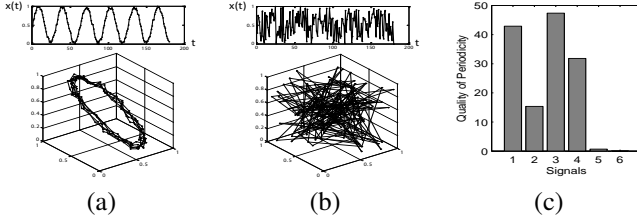


Fig. 6. The examples of TDE applied to some common signals: (a) sinusoid with noise; (b) random signal; (c) the STDE-based quality of the periodicity: 1. sinusoid; 2. sinusoid with noise; 3. sawtooth; 4. synthetic sinusoid; 5. complicated synthetic sinusoid; 6. random signal.

$s_t$  can be embedded by the observations  $o_t$ :

$$\begin{aligned} f(s_t) &= [\alpha(s_t), \alpha(s_{t-\tau}), \dots, \alpha(s_{t-(k-1)\tau})] \\ &= [o_t, o_{t-\tau}, \dots, o_{t-(k-1)\tau}], \end{aligned} \quad (2)$$

Where  $\tau$  is the lag of time-delay coordinates. A closed subset of the states  $s_t$  of the system is an attractor. This attractor  $A \subset R^d$  can be reconstructed by the the embedding k-dimension delay-vector  $[o_t, o_{t-\tau}, \dots, o_{t-(k-1)\tau}]$ . The TDE reconstruction of some common 1-D time series in 3-D space is shown in Fig. 6. As we can see, the series with simple periodicity have a simple and closed attractor, while the random signal has a mess. The readers who are interested in more details about the TDE please refer to Takens' paper [15].

2) *Proposed STDE-based Method*: TDE can help to observe the periodicity of the time series, but it does not provide the procedure on how to measure the periodicity. By observing the TDE of the signals shown in Fig. 6, some intuitive conclusions can be drawn: the more periodical the series is, (a) the shorter length the attractor has; (b) the more likely the points of the attractor lie in the same place. Based on the above two observations, an algorithm can be developed to calculate the repeatability of the time series, that is, we can calculate the linear density of shortest path in the attractor. We thus propose an enhanced TDE method, called Scored TDE (STDE), to achieve such a calculation. Its procedure is as follows:

- (1) Calculate the TDE attractor of the time series.
- (2) Pick any point of the attractor as the starting point, and select the nearest neighbor as the second point.
- (3) Repeat the same step to select the third point and the rest of points. The points can be used for only once.
- (4) Calculate the linear length  $L_s$  of the generated shortest path and the degree of periodicity:

$$Q_{STDE} = \frac{\text{Number of Points}}{L_s}, \quad (3)$$

The purpose of calculating the linear density of the shortest path instead of the direct path is to handle the case that the distance between two sequential points in a periodical series is relatively large. For instance, the series (1, -1, ..., 1, -1). The measurement of the periodicity has a few important characteristics: (1) the length of the periodic series does not affect its result; (2) the noise in the signal can seriously decrease the quality of periodicity. The quality of periodicity based on STDE method for some commonly seen signals is shown in Fig. 6 (c). It can be seen that



Fig. 7. The experiment setup (with the KineAssist robot treadmill) and the sensors.

- (1) the sinusoid and sawtooth have a quality larger than 40, and the random signal has a quality near zero;
- (2) the quality of sinusoid with light noise is half of the normal sinusoid;
- (3) the complex sinusoid containing multiple frequency components has a very low quality even it is still periodical, because it takes more effort to repeat itself.

#### D. Feet Balance Measurement

In this paper we focus on the balancing capability of patients in their rehabilitation training. Thus only the spatial distribution of the plantar pressure is considered. Four pressure sensors are placed on the insole to measure four main pressure areas of the foot, as shown in Fig. 15. These areas cover the front, back, left and right side of the foot. Fourier Transform is applied to the signal of each sensor to obtain its power spectrum, and the highest peak value in the power spectrum is chosen as the pressure level. The pressure level of these four points form a rough plantar pressure distribution of one foot, and two feet generate total eight pressure level points, which is denoted by a vector  $p$  as follows:

$$p = [p_{11}, p_{12}, p_{13}, p_{14}, p_{21}, p_{22}, p_{23}, p_{24}], \quad (4)$$

This pressure vector is directly used as the feature vector to recognize different balance situations:

- (a) which leg of the patient is weak;
- (b) whether the patient uses too much front/back or outer/inner side of foot;

## V. EXPERIMENT AND RESULTS

The experiment results are composed of three parts: motion recognition and segmentation, quality of periodicity, and feet balance measurement. The experiment platform and the sensors are shown in Fig. 7, We have designed the wireless pressure sensors. The insoles with thin film pressure sensors are put in the subject's shoes. The thermal camera is deployed right beside the treadmill.

### A. Motion Recognition and Segmentation Results

The presented PMTW is for 1-D time series data, but it could easily be generalized to high-dimensional data. The skeleton of the lower limbs extracted from the thermal images has eight skeleton nodes in the 2-D plane with  $8 \times 2 =$

16 dimensions in total. For the high-dimensional data, the matching process is implemented as follows: First, we can select a dimension with the peaks matching with the template peak pattern. For example, in our case the  $x$  displacement of ankle has a peak pattern. The peak pattern is matched with the template as shown in Fig. 9. Second, based on the matched peak pattern, we can calculate the total distance of all dimensions. Third, we can finish the rest of dimensions, as described in Sec. IV. B.

Figure 8 shows the the subject’s skeleton model in a walking cycle. The tested subject walks on the treadmill, and is asked to perform four motions: gliding, normal walking, high striding, and kicking. Gliding is to imitate the walking style of the patients with leg problems, and kicking is to test the subject’s strength. Four template series corresponding to those 4 motions are used to segment the tested series. The segmentation result is shown in Fig. 10.

Another existing segmentation algorithm, called HACA [12], is used to compare with the performance of our PMTW scheme. HACA algorithm requires input parameters before execution, such as the number of motions, the number of segments, the length of the segments. If these input parameters are close to the true values, it will have good performance. But our result indicates that HACA missed one gliding motion and confused it with the walking motion even the optimal parameters were given. Compared with other segmentation methods, PMTW does not need to define many parameters.

The typical similarity scores between the recognized segments and the template series are also shown in Fig. 10. It can be seen that all the tested motions have much higher similarity to their corresponding template series than other templates. For example, in the 1st bar chart, the recognized gliding segments has a similarity score of 0.7 to the template of gliding, and has the similarity score lower than 0.2 for all the other three templates. All the three walking style motions (gliding, normal walking, striding) have very low similarity to the kicking.

Two thresholds have been used in our algorithms: (1) The first one is in the preprocessing “amplitude smoothing”. This threshold is to eliminate the noise. In our experiment, the magnitude of the noise is smaller than half of the smallest signal. Hence the threshold is set smaller than this magnitude. (2) The second one is in the segmentation algorithm that calculates the similarity between the tested segment and the template segment. This threshold affects the recognition true positives and true negatives. After we evaluate the recognition rate, we select the similarity threshold as 0.5. As shown in the similarity score bar chart of Fig. 10, most true positives are larger than 0.6, and most true negatives are less than 0.4.

The amplitude features of selected skeleton joints in the motions from different subjects are shown in Fig. 11. The difficulty levels of performing the four motions: gliding, walking, striding, and kicking, are increased in order. It can be seen that for easy motions like normal walking, the subjects have less differences among them, and their feature clusters are separate but not so clearly distinguished. For more difficult motions like kicking, the subjects start to show more differences. And their clusters are more separate in the feature space, especially there are obvious differences in the heights of the knees. Performing

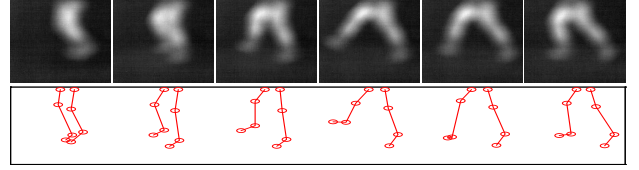


Fig. 8. The thermal images and the extracted leg skeletons in the experiment.

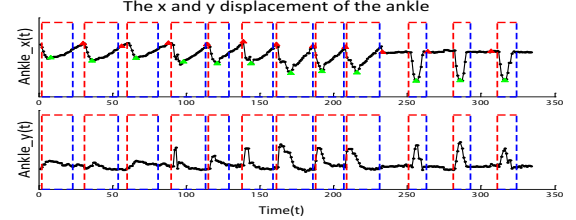


Fig. 9. The segmentation of right leg ankle motion series.

the more difficult motions can better reveal the motion ability of the tested subjects. For example, in Fig. 11 (b), the motion features of kicking divides the tested subjects into clearly different levels.

### B. Periodicity Analysis Results

The thermal camera is deployed in front of the treadmill in this experiment. We focus on the periodicity of the foot trajectory. We use the foot trajectory instead of the whole lower-limb trajectory since the foot trajectory is effective to determine the quality of periodicity of the lower-limb motions. If the foot trajectory of the subject has a high repeatability, it typically means that the subject is making good progress. The variables used for the analysis are shown in the thermal images of Fig. 12. We trace the trajectory of  $toe_x$ ,  $toe_y$ , and  $foot\ angle$ , where  $toe_x = x_1$ ,  $toe_y = y_1$ ,  $heel_x = x_2$ ,  $heel_y = y_2$ , and  $foot\ angle = \tan^{-1}((y_2 - y_1)/(x_2 - x_1))$ .

The quality of periodicity of the three variables are considered separately. In most situations, once the foot strikes on the ground, it does not move anymore. Thus we only focus on the area on which the foot strikes. Besides, the supporting foot is usually blocked by the moving leg in the thermal image. Thus in our analysis, the motion data after the foot has struck on the ground is cut off, as shown in Fig. 13.

In Fig. 13 it can be seen that the abnormal walking style is more random in both temporal and spatial domain. By using

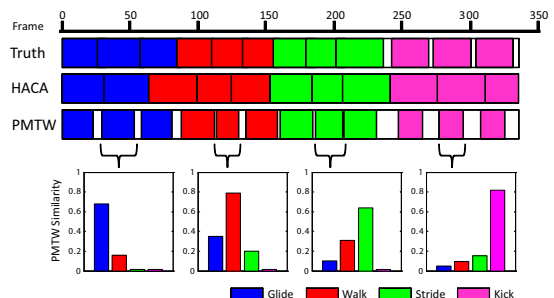


Fig. 10. The segmentation of leg motion series and the typical PMTW similarity score of the recognized segments.

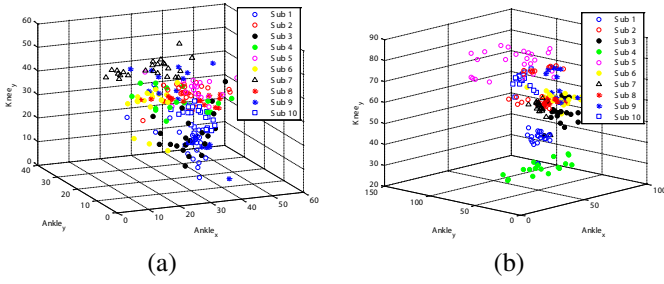


Fig. 11. The amplitude features of selected skeleton joints from different tested subjects: (a) gliding; (b) kicking.

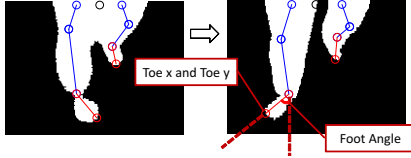


Fig. 12. The feet skeleton extracted from the thermal image.

STDE-based scheme, the spatial domain can be normalized, and the periodicity can be quantified. The time series shown in Fig. 13 are reconstructed by TDE method, as shown in Fig. 14 (a). We can see that the normal walking has more converged attractors for all the three time series. The attractors of those data look like that of sawtooth signal. The quantification result given by STDE is shown in Fig. 14 (b). The amplitude of the tested time series is around 50, which is much larger than the synthetic signals. Thus the STDE score shown in Fig. 14 (b) is normalized for better consistence with Fig. 6 (c). This bar chart shows that the quality of periodicity of the abnormal waling is about half of the normal walking for all three variables.

### C. Plantar Pressure Results

In this experiment the thin film force sensors FlexiForce A201 from Tekscan are used to measure the pressure under the feet. The specification of the sensor is given in Table I.

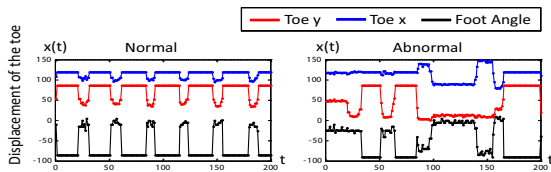


Fig. 13. The comparison of time series of the foot motion between normal walking and abnormal walking (pixel as amplitude unit).

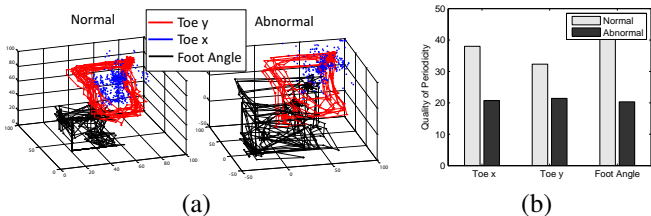


Fig. 14. The comparison of STDE-based result for the foot motion: (a) in the reconstruction space; (b) scored quality of periodicity.

TABLE I  
SPECIFICATION OF THE FLEXIFORCE FORCE SENSOR.

Thickness	0.008 in.	Sensing Area	0.375 in. diameter
Length	7.5 in.	Standard Force Ranges	445 N (0 - 100 lb)
Width	0.55 in.	Response Time	< 5 $\mu$ sec

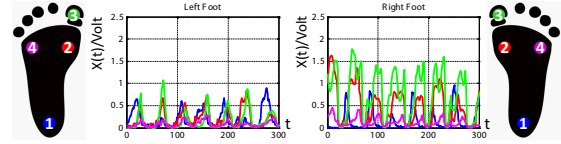


Fig. 15. The pressure signals when the left leg is disabled.

The sampling rate of the pressure sensor is 25 Hz. The time series of the pressure signals for a subject with disabled left foot is shown in Fig. 15. The pressure distribution generated from the power spectrum is shown in Fig. 16. The pressure level is normalized within the eight pressure levels. The color and the number indicate the pressure positions, as shown in Fig. 15. The pressure distribution shows that:

- the area near tiptoe sustains the largest pressure load in normal walking;
- when one leg of the subject is disabled, the corresponding foot still sustains pressure, but the pressure is concentrated on a small area of the foot. And the available foot is also influenced, because the imbalance between two feet has impact on the function of both feet;
- when the subject walks on his toes, most of the pressure goes to the front foot;
- when the subject walks on his outer edge of the feet, the pressure is concentrated on the two sides of the foot.

By studying different walking cases, we find that area 3 on the foot always supports the body unless one walks on his heel. Using the pressure feature vector in Eq. 4, the balancing capability of the subject can be classified. These feature vectors are originally strong, so we use direct classification: First, calculate the distance between the tested feature vector and the model feature vector. Second, the tested feature vector is recognized as one of the models if its distance to that model is smallest among all models. The classification performance is shown in Fig. 17. There is little misclassification between the disabled left leg walking and the normal walking 2, the reason may be that subject 2 tends to use more of his left leg in the tests. For other situations, the classification performs well.

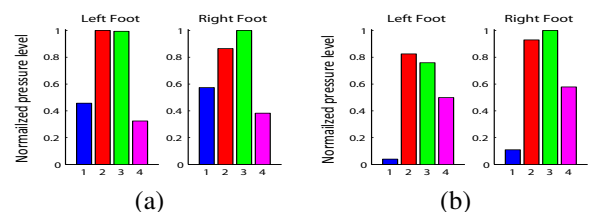


Fig. 16. The normalized distribution of plantar pressure under different cases: (a) normal; (b) walk on toe.

	Normal 1	Normal 2	Normal 3	On toe	On outer edge	Right leg disabled	Left leg disabled
Normal 1	0.98	0.13	0.35	0	0	0	0
Normal 2	0.23	0.88	0	0	0	0	0.25
Normal 3	0.28	0.03	0.88	0	0	0.01	0.08
On toe	0	0	0	0.95	0	0	0
On outer edge	0	0	0	0	0.9	0	0
Right leg disabled	0	0	0.03	0	0	0.83	0
Left leg disabled	0.03	0.35	0.18	0	0	0	0.88

Fig. 17. The confusion matrix of the classification of the foot balance.

	Glide	Walk	Stride	Kick
Glide	0.97	0	0	0
Walk	0	0.92	0.33	0
Stride	0	0.10	0.89	0
Kick	0	0	0	1

(a)

	Glide	Walk	Stride	Kick
Glide	0.44	0.21	0	0
Walk	0.32	0.83	0	0
Stride	0	0	0.90	0
Kick	0.21	0.81	1	0.56

(b)

	Glide	Walk	Stride	Kick
Glide	0.91	0	0	0
Walk	0.26	0.86	0	0
Stride	0	0.14	0.85	0
Kick	0	0	0	1

(c)

Fig. 18. The confusion matrix of the recognition performance: (a) Accelerometer system; (b) GEI based method; (c) PMTW scheme;

#### D. Comparison with Other Systems

(1) CC2540 BLE device with 3-axis accelerometers, CMA3000d, is used in the experiments. The recognition performance comparison result is shown in Fig. 18. It can be seen that IMU sensors have good recognition rate except that the walking is a little confused with striding. However, we did not use IMU sensors in our system because they cannot measure the absolute values of human posture such as the angle of the knee. Those absolute values can be captured by the thermal camera.

(2) The existing thermal camera systems are quite expensive. For example, Xue et al. [6] use Flir A40M which costs \$14K. It has a 320x240 resolution and a 60Hz frame rate, and weighs several pounds. Our system Therm-App has a 384x288 resolution and only 9 Hz frame rate, but it is good enough to capture the motions of patients under rehabilitation training. Also, the existing thermal camera systems cannot segment the motion series automatically in real-time. In the work [6], gait energy image (GEI) based method is used for the recognition. The comparison with GEI is also given in Fig. 18. As we can see, the GEI method has poor performance in terms of differentiating the four motions, while our PMTW scheme has small confusions among them.

(3) MMS Kinect can detect everything in the field of view. In our application, the treadmill and the bands supporting the subject, become obstacles in the depth image, as shown in Fig. 19. MS Kinect cannot capture the images well due to those obstacles. While the thermal camera will not be affected by them. Moreover, the original Kinect SDK cannot recognize the human skeleton, and the extra image processing takes large computation overhead.

## VI. CONCLUSIONS

This paper has presented an intelligent sensing system for the quantitative assessment of the motion quality in lower-limb rehabilitation training. The system used portable thermal camera and wireless sensors to collect lower-limb motion data from the subjects. We have developed a series of fast

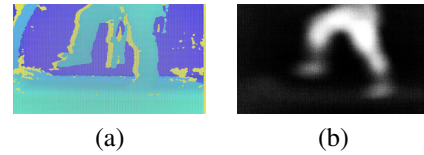


Fig. 19. The comparison of detection performance: (a) MS Kinect depth image; (b) thermal image.

algorithms to process the sensor data. To recognize and segment the motion series, we have developed PMTW-based algorithm to match the time series and calculate the similarity between them. To assess the quality of periodicity of human motions in rehabilitation training, we have developed STDE-based method to define the motion repeatability. Little work has been done in this area. For the feet balance evaluation, we have utilized the spatial distribution of the plantar pressure data.

## REFERENCES

- [1] Stroke statistics, please see: <http://www.uhnj.org/stroke/stats.htm>
- [2] Y.L. Hsu, P.C. Chung, W.H. Wang, M.C. Pai, C.Y. Wang, C.W. Lin, H.L. Wu, J.S. Wang, "Gait and Balance Analysis for Patients With Alzheimer's Disease Using an Inertial-Sensor-Based Wearable Instrument," *IEEE J. Biomed. Health Inform.*, vol. 18, no. 6, pp. 1822-1830, Nov. 2014.
- [3] R. Ayase, T. Higashi, S. Takayama, S. Sagawa, and N. Ashida, "A method for supporting at-home fitness exercise guidance and at-home nursing care for the elders, video-based simple measurement system," *10th IEEE Intl. Conf. on e-Health Networking, Applications and Service (HEALTHCOM 2008)*, pp.182-186, July 2008.
- [4] I. Ar and Y.S. Akgul, "A Computerized Recognition System for the Home-Based Physiotherapy Exercises Using an RGBD Camera," *IEEE Trans. Neural Syst. Rehabil. Eng.*, vol. 22, no. 6, pp. 1160-1171, Nov. 2014.
- [5] S. Das, L. Trutoiu, A. Murai, D. Alcindor, M. Oh, F.D. Torre, and J. Hodgins, "Quantitative measurement of motor symptoms in Parkinson's disease: A study with full-body motion capture data," *2011 Annual International Conference of the IEEE Engineering in Medicine and Biology Society (EMBC)*, pp. 6789-6792, Aug. 2011.
- [6] Z. Xue, D. Ming, W. Song, B. Wan, and S. Jin, "Infrared gait recognition based on wavelet transform and support vector machine," *Pattern Recognition*, vol 43, Issue 8, pp. 2904-2910, Aug. 2010.
- [7] Thermal camera introduction, please refer to <http://therm-app.com/>.
- [8] D.L. Jaffe, D.A. Brown, C.D. Pierson-Carey, E.L. Buckley, and H.L. Lew, "Stepping over obstacles to improve walking in individuals with poststroke hemiplegia," *Journal of Rehabilitation Research & Development*, vol. 41, no. 3A, pp. 283-292, May-June 2004.
- [9] J.F.-S. Lin, D. Kulic, "Online Segmentation of Human Motion for Automated Rehabilitation Exercise Analysis," *IEEE Trans. Neural Syst. Rehabil. Eng.*, vol. 22, no. 1, pp. 168-180, Jan. 2014.
- [10] J. Frank, S. Mannor, J. Pineau, D. Precup, "Time Series Analysis Using Geometric Template Matching," *IEEE Trans. Pattern Anal. Mach. Intell.*, vol. 35, no.3, pp. 740-754, March 2013.
- [11] E. J. Keogh and M. J. Pazzani, "Derivative dynamic time warping," *SIAM Int. Conf. on Data Mining (SDM)*, pp. 1C11, 2001.
- [12] F. Zhou, F.D. Torre, and J.K. Hodgins, "Hierarchical Aligned Cluster Analysis for Temporal Clustering of Human Motion," *IEEE Trans. Pattern Anal. Mach. Intell.*, vol. 35, no. 3, pp. 582-596, March 2013.
- [13] F. Liu, R.W. Picard, "Finding periodicity in space and time," *Sixth International Conference on Computer Vision*, pp. 376-383, Jan. 1998.
- [14] Post-stroke rehabilitation effect measurement: <http://www.neuropt.org/professional-resources/neurology-section-outcome-measures-recommendations/stroke>
- [15] F. Takens, "Detecting strange attractors in turbulence," *Dynamical Systems and Turbulence, Warwick 1980*, vol. 898, no.3, pp. 366-381, 1981.